Available online at www.eccomasproceedia.org
Eccomas Proceedia COMPDYN (2021) 4621-4632

ECCOMAS
Proceedia

COMPDYN 2021
8th ECCOMAS Thematic Conference on
Computational Methods in Structural Dynamics and Earthquake Engineering
M. Papadrakakis, M. Fragiadakis (eds.)
Streamed from Athens, Greece, 28 - 30 June 2021

INTENSITY MEASURES PROPERTIES AND SELECTION FOR RISK ANALYSIS ON STRUCTURES SUBJECTED TO EARTHQUAKE INDUCED POUNDING WITH A NON-SMOOTH CONTACT DYNAMICS METHOD

T. Langlade[1], D. Bertrand[1], S. Grange[1], G. Candia[2], and J.C. De La Llera[3]

[1]Laboratory GEOMAS EA7495
INSA Lyon, Villeurbanne, France
e-mail: {thomas.langlade,david.bertrand,stephane.grange}@insa-lyon.fr

[2] Research Center for Integrated Disaster Risk 5 Management (CIGIDEN), ANID/FONDAP/15110017
Facultad de Ingenieria, Universidad Del Desarrollo, Santiago de Chile, Chile
e-mail: gacandia@gmail.com

[3] Research Center for Integrated Disaster Risk 5 Management (CIGIDEN), ANID/FONDAP/15110017
Pontificia Universidad Catolica de Chile, Santiago de Chile, Chile
e-mail: jcllera@ing.puc.cl

Abstract. *This study aims at selecting the best suited Intensity Measures (IMs) in the case of earthquake-induced building pounding to plot fragility functions of civil engineering structures. IMs are indicators representative of the seism "intensity" (e.g. the magnitude, the Peak Ground Acceleration (PGA)) that are intended to be correlated with Engineering Demand Parameters (EDPs) of interest (e.g., interstory drift, shear force). Desirable properties of IMs are efficiency (i.e., the predictability of the EDP for a given IM), and sufficiency (i.e., the independence of the prediction regarding Ground Motions Parameters (GMPs)) on magnitude and source-to-site distance. The study is achieved by means of 1677 Ground Motions (GMs) computed on two Single Degrees Of Freedom (SDOFs) whose modal characteristics are fitted with real-size structures. The numerical treatment of the contact is achieved with the Non-Smooth Contact Dynamics (NSCD) method which showed very good capabilities of reproducing the expected occurrence and number of impacts. Once one or several IMs are considered both efficient and sufficient enough, a future work will compute fragility and risk curves of these adjacent pounding SDOF with various separation distances.*

Keywords: Earthquake induced Building-Pounding, Intensity Measures, Non-Smooth Contact Dynamics, Efficiency-Sufficiency properties

ISSN:2623-3347
Peer-review under responsibility of the organizing committee of COMPDYN 2021.
doi: 10.7712/120121.8812.18557

1 INTRODUCTION

Earthquake-induced building pounding occurs typically in densed urban areas where low to mid-height buildings are more likely to be adjacent. Field reports, experimental campaigns, and numerical analysis, have shown and demonstrated the potential negative effects of impact between structures, ranging from minor architectural damages [1, 2], to significant increases in interstory drifts [3, 4] and ductility demand [5, 6], to, in rare occasions, collapse [7]. Figures 1a and 1b illustrate respectively the aftermaths of building pounding in Mexico and Turkey.

(a) Mid-story floor collapse of Hotel de Carlo in Mexico City (Mw 8.1 earthquake) [8]

(b) Pounding damage (Mw 7.4, Izmit earthquake, Turkey, 1999) [9]

Figure 1: Building pounding damage during earthquakes

Building codes such as Eurocode 8 [10] give recommendations on separation distance between adjacent buildings, but they are either too conservative leading to unused land space, or contact occurs due to both large ground motions and buildings uncertainties. Considering the increasing world urban densification, it is acceptable to say that building pounding will continue happening.

Predicting the effects of such phenomenon in engineering design is of importance, especially throughout the lifetime of a given building in a precise geographical and urbanized environment. The purpose of the PBEE (Performance-Based Earthquake Engineering) framework [11] is to assess numerically the IMs correlations with some EDPs of interest. Most often, the IMs chosen are hazard curves of pseudo-acceleration at the structure fundamental period [12]. Probabilities and return periods of critical events are then computed from the statistical data from the studied region. To a further length, damage measures (service state, close to collapse, necessary repairs,...) and decision variables (cost, life,...) can be successively evaluated. Such information is of importance during new phases of life of a project (*e.g.* building design, renovation and expansion) to help decision-makers. To do so, IMs and EDPs are to be correlated for the chief executives to trust the predictions. A trusted IM should then properly reproduce with a reduced variability the EDP value and be conditionally independent on GMPs such as source-to-site distance and magnitude. An efficient and sufficient IM also requires reliable attenuation relationships, or Ground Motion Prediction Equations (GMPEs) to produce trustworthy risk curves. IMs efficiency and sufficiency properties through earthquake and impact are investigated in this paper.

Today, fast (in terms of computational time), robust and ergonomic numerical tools are required in order to run these probabilistic seismic risk analysis. The contact formulation needs

appropriate treatment; classical penalty approaches might give scattered results due to the sensitivity of its parameters [13]. This study uses an alternative way by the use of the Non-Smooth Contact Dynamics (NSCD) method [14, 15]. First, its capabilities are introduced with an idealized test-case. Secondly, a comparison between the experimental and numerical displacements of colliding structures on a shaking table (scale 1:1, EMSI laboratory at CEA Saclay in the frame of national project ANR SINAPS [4, 16]) allows validating the efficiency and robustness of the NSCD method and its use in the efficiency-sufficiency analysis. To the knowledge of the authors, no NSCD-based risk analysis has been carried out in the literature.

2 CAPABILITIES OF THE NSCD METHOD

The works by Moreau [17], Jean [14], and Acary [15, 18] have proven the energy conservation, the accuracy, and the application of the NSCD method in finite elements methods. It uses a Moreau-Jean integration scheme associated with a Newton impact law. It allows to apply an instantaneous change in velocities of the nodes in contact. This method has the advantage to depend only on the sole coefficient of restitution e taken between 0 and 1; it represents the system energy dissipation upon contact.

2.1 Test case : two impacting structures with no energy loss

To illustrate NSCD capabilities, a test case involving impact is presented. Two similar SDOFs named Structure 1 and Structure 2 with fundamental periods T_1 and T_2 both equal to 1s are set adjacent to one another with a null separation distance. They are both subjected to an initial velocity V_1 and V_2 of 1m/s shoving them away in opposite senses before going backwards and impact. Figure 2 presents the set-up. No damping is considered, and the coefficient of restitution equals 1. This way, structures are meant to collide perpetually every 0.5s.

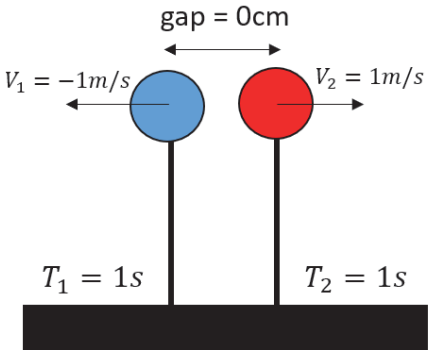

Figure 2: Structures 1 and 2 at initial state for test case

Figure 3 presents the displacements (upper figure) and velocities (lower figure) of the system. The kinematics behaves exactly as expected with a instantaneous change in velocities upon contact, no damping is observed, and collisions are indefinitely perpetuated.

2.2 Scale 1:1 reinforced concrete impacting slabs

Ph.D work of Crozet [16] involved the study of scale 1:1 structures colliding both in free motion or subjected to a seismic solicitation. Two instrumented reinforced concrete slabs of 4.6

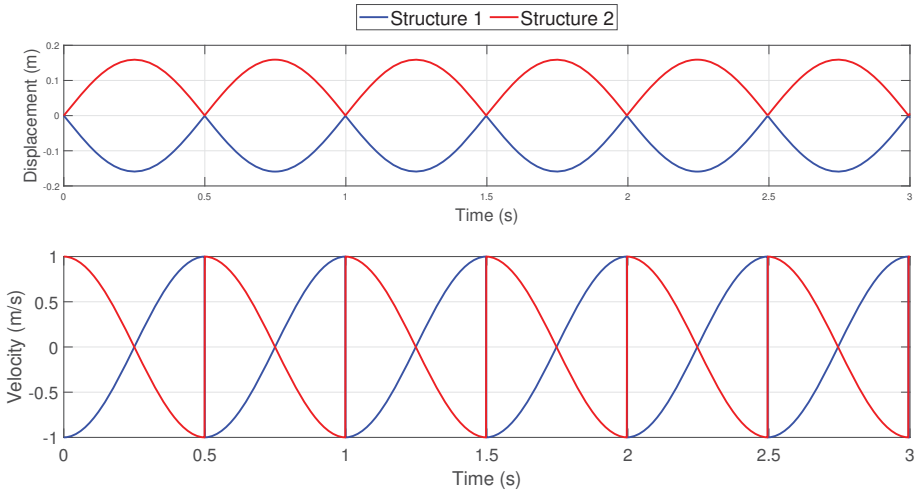

Figure 3: Impacting structures : test case with no damping

tons and 3.5 tons were mounted respectively on four 2.5m high steel HE100AA and HE140AA columns and set a few centimeters next to each other on a shaking table. Additional elements can be added to these single-story structures to make them two-story high, as shown by Figures 4a and 4b. Nevertheless, it is not the case of the present work where only the single-story set-up is considered because behaving like SDOFs. Structures are named 1 and 2, behave in linear elastic fashion, and have respectively their fundamental period equal to 0.28s (heavier, more flexible) and 0.15s (lighter, stiffer).

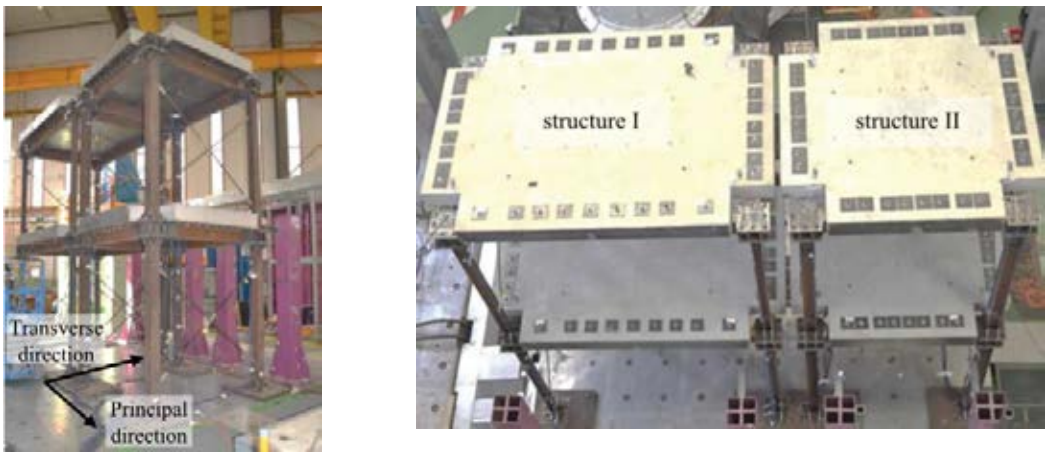

(a) (b)

Figure 4: Structure 1 and Structure 2 set on the shaking table [16, 4]

Figure 5 presents the comparison of the experimental outcomes with the numerical model. The coefficient of restitution e equals 0.6. The comparison shows excellent agreement between the expected and numerical displacements, both in terms of kinematics, and time occurrence of impacts. Only one impact is not reproduced at 9.5s. Even if structures visually seem to collide more, especially between 11s and 14s, the accelerometers set up on the slabs did not detect more contacts.

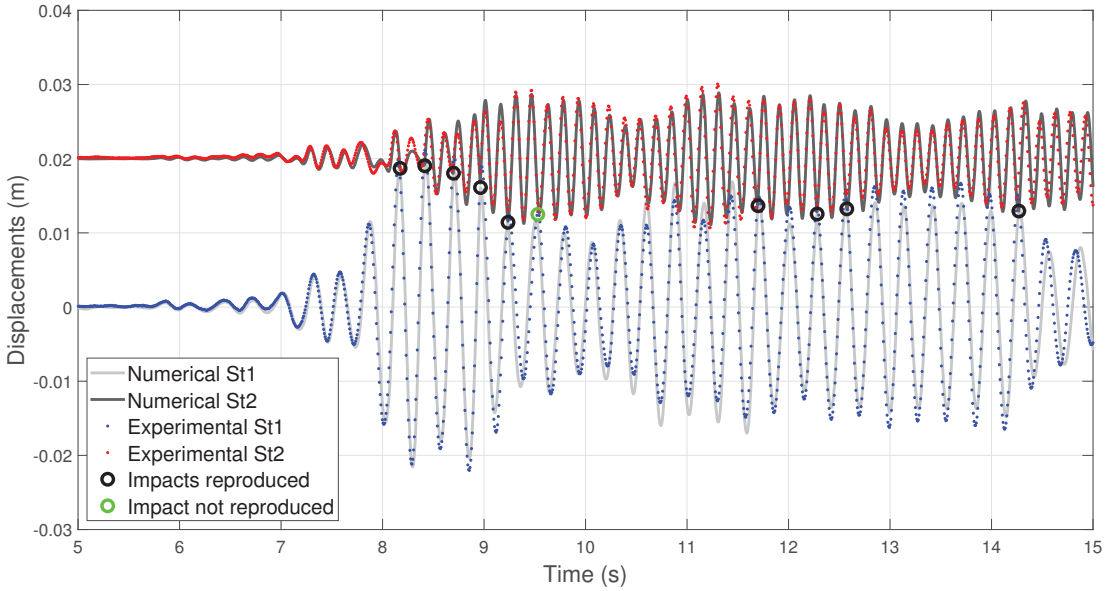

Figure 5: Cadarache 0.25g : Numerical versus Experimental comparison

Additional kinematic and spectral analysis produced very good results that confirmed $e = 0.6$ is a value of interest in the frame of parallel colliding reinforced concrete slabs, but are not presented in the current work. To reduce the computation cost, the efficiency and sufficiency analysis are run with the structures modelled as SDOFs calibrated on the experimental data.

3 IMs EFFICIENCY AND SUFFICIENCY PROPERTIES

This section presents successively the list of IMs that are studied, the GM database, the coefficients used to assess the efficient and sufficient properties, and a discussion on the various gaps studied. Henceforth, the EDP chosen to deduce IM properties is the interstory drift δ.

3.1 List of IMs

Six IMs are investigated, the pseudo-acceleration at the fundamental period T_f of the structure $S_a(T_f)$, the PGA, the Arias Intensity (AI), the Cumulative Absolute Velocity (CAV) and Standard CAV ($SCAV$), and the averaged pseudo-acceleration $S_{avg}(T_f)$. Considering that earthquake-induced building pounding necessarily involves two buildings, $S_a(T_f)$ and $S_{avg}(T_f)$ are studied for T_f equal both to T_1 and T_2, the respective fundamental periods of the Structure 1 and 2. Table 1 lists the six IMs studied throughout this work.

3.2 Ground Motion set: Siber-Risk database

The 1677 GM extracted from the Siber-Risk database [19] comply with the properties presented by Table 2. This selection is consistent with the geographic location of the Valparaiso city in Chile. Interface types earthquakes (rupture zone located above 60km under the earth surface) are the most frequent, and the shear velocity in 30 meters below the ground surface Vs30 is a class C type soil (very dense). Only ground motions of magnitude greater than five are selected, the authors considering that no significant damages are produced with smaller magnitudes.

IM	Formulation	Notes
$S_a(T_f)$	pseudo-spectral acceleration at T_f	T_f : fundamental period
PGA	$max(\|a(t)\|)$	$a(t)$: acceleration time history
AI	$\frac{\pi}{2g}\int_0^{t_f} a(t)^2 dt$	g = 9.81 m/s² t_f : seism time duration
CAV	$\int_0^{t_f} \|a(t)\| dt$	t_f : seism time duration
$SCAV$	$SCAV = CAV_i + \int_{t_{i-1}}^{t_i} \|a(t)\| dt$	$a(t)$: acceleration in one-second interval where at least one value is greater than 0.025g i = 1,...,N_r with N_r the record length in seconds
$S_{avg}(T_f)$	$(\prod_{i=1}^{N} S_a(c_i T_f))^{1/N}$	T_f : fundamental period Scalars c_i : $c_1 = 0.5 \leq ... \leq 1 \leq ... \leq c_N = 2$ N : length of $[c_1 T_f, ..., T_f, ..., c_N T_f]$

Table 1: List of IMs studied

GMP	Min. Value	Max. Value
Magnitude	5	8.8
Vs30	360	800
Type	Interface	

Table 2: GM selection for the Valparaiso region (Chile)

3.3 Efficiency

The efficiency of an IM regarding a peculiar EDP is assessed with both the Coefficient Of Variation (COV) and the regression coefficient (R^2). The first represents the variability around the mean value of the distribution (*i.e.* Eq.(1) where σ is the standard deviation, and μ the mean value of the distribution). Unlike σ, COV has no dimension which is useful when comparing the efficiency property between EDPs of different natures.

$$COV = \frac{\sigma}{\mu} \tag{1}$$

R^2 represents how much the logarithmic EDP-IM correlation is linear, and is calculated directly from a software. A $R^2 = 1$ value indicates a perfect linear relationship. Henceforth, an IM is arbitrary considered "efficient enough" if $COV \leq 0.10$ and $R^2 \geq 0.90$.

3.4 Sufficiency

The sufficiency of IMs is commonly calculated regarding the source-to-site distance (*i.e.*, herein, the distance to the rupture fault) and the magnitude of the GM. The results of the present study are independent of the soil conditions (see Vs30 range in Table 2) and the earthquakes nature (Interface type) accordingly to the selected dataset. Non-exhaustively, the fault rupture mechanism, the directivity of the earthquakes, and the ϵ coefficient [12] representing the ran-

domness of the GM are not considered in this study.

Two ways of assessing the sufficiency to magnitude and distance are studied. The p-value "p" (statistical F-test) delivers a binary assessment of the IM, considering it either sufficient if $p \geq 0.05$ or not sufficient if $p \leq 0.05$. This parameter has been notably used by Luco and Cornell [20], and Eads and Miranda [21, 22] in the civil engineering field. This parameter is calculated through a calculation software. The second sufficiency coefficient is the Spearman rank coefficient ρ presented by Eq.(2).

$$\rho = 1 - \frac{6 \sum_{i=1}^{N} D^2}{N(N^2 - 1)} \tag{2}$$

With D the differences between the ranks of the N dataset values. ρ measures how much the data fits with a monotonic relationship. ρ is between -1 and 1, representing respectively a perfect negative linear dependency, and a perfect positive linear dependency. A $|\rho|$ close to zero denotes the IM is independent from the GMP.

Unlike the p-test, the Spearman coefficient does not produce a binary evaluation of the sufficiency, but it allows a relative comparison of this property, enabling a classification of IMs. To the knowledge of the authors, no risk analysis of building pounding has been carried out with both p-value and Spearman coefficients. $p(M)$, $p(D)$, $\rho(M)$, and $\rho(D)$ are respectively the p-value and Spearman coefficients calculated for magnitude and distance for a given couple of EDP and IM. Henceforth, an IM is considered sufficient if $p(M)$ and $p(D)$ are, by definition, greater than 0.05 and if $|\rho(M)|$ and $|\rho(D)|$ are arbitrary less than 0.10 (De Biasio [23] considered the IM sufficient if $|\rho| \leq 0.20$).

4 RESULTS

One important issue of the building pounding study is the gap separation. Each gap separation chosen consists in itself in a whole single system. For instance, if 11 gaps are studied, then the outcomes to analyse are multiplied by 11 ; *i.e.*, it means first computing 11 times 1677 GM on the structures, retrieving 11 times 1677 EDPs, and inferring 11 times the efficient-sufficient coefficients. The analysis of six coefficients of eight IMs for two structures separated by 11 different gaps is important in terms of computation time. In this work, authors decided to rather obtain a general overlook by averaging the efficient-sufficient coefficients over all the gaps. Thus, the amount of data to analyse is reduced by a factor 11. First, an example is given with the coefficients R^2 and COV of $S_a(T_1)$ for Structure 1. Secondly, all efficiency-sufficiency coefficients for both structures are presented.

4.1 Example of the average of R^2 and COV coefficients $S_a(T_1)$ relationship

Figure 6b presents the interstory drift δ_1 plots against the $S_a(T_1)$ of Structure 1, in logarithmic scale, and for both a 5mm and infinite (no-collision case) separation distance. Only the ground motions that actually produced collision in the five millimeters case are plotted.

As expected without contact in a elastic linear structure, a perfect linear fit links the interstory-drift with $S_a(T_1)$ (*i.e.*, magenta dots and green line are superposed), R^2 and COV are respectively equal to 1 and 0. On the contrary, the efficiency properties are lesser when impact is

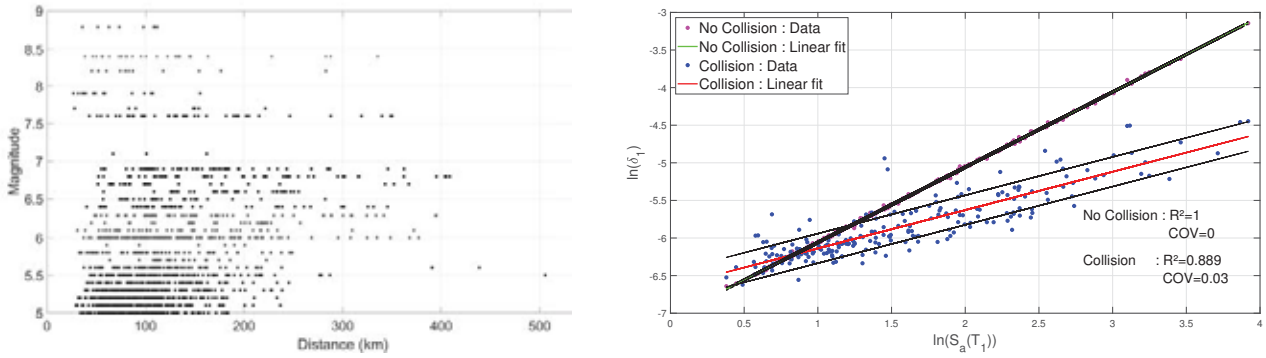

(a) (b)

Figure 6: (a) Selected Database : 1677 GM (b) Outcomes of Structure 1 with gap = 5mm

involved with gap=5mm. At this distance, 227 out of the 1677 GM produced impact, resulting in R^2 and COV respectively equal to 0.89 and 0.03 (*i.e.*, blue dots are scattered around the red linear curve). Thus, for each gap studied, R^2 and COV will have different values.
As an example, Table 3 presents the COV results for $S_a(T_1)$ for N=11 separation distances. N_g^{GM} corresponds to the number of GM inducing collision for the gap indexed g.

Gaps (mm)	0	1	2	3	4	5	6	7	8	9	10
Index g=1,...,N=11	1	2	3	4	5	6	7	8	9	10	11
N_g^{GM}	1677	1020	575	395	297	227	182	148	128	113	106
$S_a(T_1)$: R_g^2	0.90	0.91	0.91	0.91	0.91	0.89	0.88	0.85	0.82	0.79	0.82
$S_a(T_1)$: COV_g	0.06	0.04	0.04	0.03	0.03	0.03	0.03	0.04	0.04	0.04	0.03

Table 3: $S_a(T_1)$: R^2 and COV values of Structure 1

As expected for a gap null, all 1677 simulations induce impact and the number decreases as the gap increases. At 10mm the number drops to 106 which was decided to be the larger and last gap computed since (i) it is almost the same number (113) as for gap=9mm (ii) it is less than 10% of the totality of the database. In this study case, R^2 decreases from 0.90 to 0.82 (important loss of efficiency) while COV decreases from 0.06 to [0.03;0.04] (small gain of efficiency) when the gap increases from zero to 10mm.

Let's now note R_g^2 and COV_g respectively the regression coefficient and coefficient of variation for the g identified gap (Table 3). All R_g^2 and COV_g are then averaged and weighted by N_g^{GM}, the number of ground motions that actually induced collision for the gap number g; let's note the results respectively R_{avg}^2 and COV_{avg}. Eq.(3) presents the formulation used with R_{avg}^2. Eq.(4) and Eq.(5) respectively present the numerical application for R^2 and COV_{avg} for $S_a(T_1)$. These values can be found in the third column, at the third and fourth lines of Table 4.

$$R^2_{avg} = \frac{\sum_{g=1}^{N=11} R^2_g N^{GM}_g}{\sum_{g=1}^{N=11} N^{GM}_g} \tag{3}$$

$$R^2_{avg} = \frac{0.90 * 1677 + 0.91 * 1020 + ... + 0.82 * 106}{1677 + 1020 + ... + 106} = 0.90 \tag{4}$$

$$COV_{avg} = \frac{0.06 * 1677 + 0.04 * 1020 + ... + 0.03 * 106}{1677 + 1020 + ... + 106} = 0.043 \tag{5}$$

4.2 Identification of the most efficient-sufficient IMs

Tables 4 and 5 present respectively for Structure 1 and Structure 2, the averaged values of the efficiency-sufficiency coefficients. The values are bold if the IM complies with the criterion of validity.

	Validity Criterion	$S_a(T_1)$	PGA	AI	CAV	$SCAV$	$S_{avg}(T_1)$
R^2	≥ 0.90	**0.90**	0.87	0.89	0.82	0.82	**0.92**
COV	≤ 0.05	**0.043**	**0.046**	**0.043**	0.055	0.054	**0.036**
$p(M)$	≥ 0.05	**0.37**	6e-6	**0.208**	**0.074**	**0.211**	0.044
$\lvert\rho(M)\rvert$	≤ 0.10	**0.042**	**0.049**	**0.046**	**0.028**	**0.041**	**0.024**
$p(D)$	≥ 0.05	**0.66**	**0.13**	**0.41**	0.002	0.002	**0.13**
$\lvert\rho(D)\rvert$	≤ 0.10	**0.048**	**0.037**	**0.029**	**0.041**	**0.039**	**0.030**

Table 4: Structure 1 : Averaged IMs coefficients of Efficiency-Sufficiency

Efficiency: For both structures, $S_{avg}(T_f)$ is the most efficient IM, their respective R^2 and COV respectively plainly greater and smaller than all the other IMs coefficients. $S_a(T_f)$, PGA, and AI show good efficiency properties although closer to the validity criterion than $S_{avg}(T_f)$, or even not compliant with the criterion for Structure 2. CAV and $SCAV$ are clearly not efficient enough in the regard of that study case.

Sufficiency: $S_a(T_f)$, AI, and $S_avg(T_f)$ are conditionally independent on magnitude and distance parameters for Structure 1, it is validated by both the p-value and Spearman ranking coefficients. PGA only misses the $p(M)$ to have also a complete sufficiency validation. The Spearman coefficients of $S_{avg}(T_f)$ are overall smaller than $S_a(T_f)$, implying a better sufficiency.

	Validity Criterion	$S_a(T_2)$	PGA	AI	CAV	$SCAV$	$S_{avg}(T_2)$
R^2	≥ 0.90	0.88	**0.91**	**0.90**	0.82	0.82	**0.94**
COV	≤ 0.05	**0.048**	**0.042**	**0.044**	0.06	0.057	**0.034**
$p(M)$	≥ 0.05	**0.459**	0.011	7e-5	2e-4	2e-4	**0.087**
$\|\rho(M)\|$	≤ 0.10	**0.069**	**0.036**	0.054	**0.036**	**0.025**	**0.028**
$p(D)$	≥ 0.05	**0.77**	**0.29**	0.001	5e-5	4e-5	**0.32**
$\|\rho(D)\|$	≤ 0.10	**0.046**	**0.029**	**0.040**	**0.044**	**0.027**	**0.051**

Table 5: Structure 2 : Averaged IMs coefficients of Efficiency-Sufficiency

5 CONCLUSIONS

This article presents the methodology for evaluating the properties of efficiency (predictability of the EDP for a given value of IM) and sufficiency (conditional independence of the IM regarding chosen GMP, herein magnitude and distance) of six IMs in the building pounding framework. It aims to select the best suited IM among $S_a(T_f)$, PGA, AI, CAV, $SCAV$, and $S_{avg}(T_f)$ in the case of risk-assessment studies on elastic buildings colliding at their slab levels. Two different tests, p-value's and Spearman rank's, are used to enforce the conclusions.

The NSCD method used for contact detection and treatment on two SDOFs has produced excellent agreement with both an idealized test case (Figures 2 and 3), and the experimental data extracted from real size colliding structures (Figure 4). These tests validated the NSCD method use in the 1677 GM from the Siber-Risk database are computed on the numerical model for six different gaps as displayed by Table 3. The efficiency-sufficiency coefficients inferred from each gap study are then averaged and weighted (Eq.(3)) to obtain an overview of the IMs properties in this system configuration (two parallel colliding reinforced concrete slabs).

$S_{avg}(T_f)$ is the most efficient IM for the two structures and shows very good sufficiency properties relatively to the other IMs. Although with less interesting grades than $S_{avg}(T_f)$, the IMs $S_a(T_f)$, PGA follow close behind. AI checks all the cases for Structure 1, but falls short on the p-value test of magnitude and distance for Structure 2. Finally, CAV and $SCAV$ are discarded for far behind all the aforementioned IMs.

The continuation of this work is the computation of fragility and risk curves; the first giving the probability of exceeding an EDP value of interest for a given value of IM, the second being the convolution of the first with hazard curves [12]. $S_{avg}(T_f)$ is then the best candidate for fragility curves. For risk curves on the other hand, the more widely known the IM is, the larger the number of existing GMPEs is, and the more accurate and consensual the hazard curves are. In this regard, scientists have more experience using $S_a(T_f)$ and PGA rather than $S_{avg}(T_f)$ whose GMPEs are smaller in number.

ACKNOWLEDGEMENTS

This work is partly founded by a CDSN Grant (Contrat Doctoral Spécifiques aux Normaliens) and the ECOS-Sud Grant for international collaboration CONICYT-ECOS170044. The authors deeply thanks V. Crozet of the French CEA for the provisioning of the experimental data [13]. Many thanks are also addressed to V. Acary and F. Bourrier respectively of the INRIA (Institut National de la Recherche en sciences et technologies du numérique) and INRAE (Institut National de la Recherche pour l'Agriculture, l'alimentation et l'Environnement) for their guidance into the NSCD method use. In addition, this work has been partially developed within the framework of the federative project I-RISK (L'offre de solutions au traitement des risques naturels) co-funded by the European Union (FEDER) and "La région Auvergne-Rhône-Alpes" which aims at proposing innovative solutions for natural hazards mitigation.
Dr. Candia received support from Facultad de Ingenieria Civil at Universidad del Desarrollo - Chile, FONDECYT Grant 11180937 "Seismic Risk of Mined Tunnels", the National Research Center for Integrated Natural Disaster Management FONDAP/CIGIDEN 15110017, and FONDECYT Grant Number 1170836, "SIBER-RISK: SImulation Based Earthquake Risk and Resilience of Interdependent Systems and NetworKs." The authors are grateful for this support.

REFERENCES

[1] Gregory Cole, Rajesh Dhakal, Athol Carr, and Des Bull. Interbuilding pounding damage observed in the 2010 Darfield earthquake. *Bulletin of the New Zealand Society for Earthquake Engineering*, 43(4):382–386, December 2010. Number: 4.

[2] V Jeng and W. L Tzeng. Assessment of seismic pounding hazard for Taipei City. *Engineering Structures*, 22(5):459–471, May 2000.

[3] SA Anagnostopoulos. Building pounding re-examined: How serious a problem is it? 11th World Conference on Earthquake Engineering, 1996.

[4] Vincent Crozet, Ioannis Politopoulos, and Thierry Chaudat. Shake table tests of structures subject to pounding. *Earthquake Engineering & Structural Dynamics*, 48(10):1156–1173, 2019. _eprint: https://onlinelibrary.wiley.com/doi/pdf/10.1002/eqe.3180.

[5] Maria J. Favvata. Minimum required separation gap for adjacent RC frames with potential inter-story seismic pounding. *Engineering Structures*, 152:643–659, December 2017.

[6] Chris G. Karayannis and Maria J. Favvata. Earthquake-induced interaction between adjacent reinforced concrete structures with non-equal heights. *Earthquake engineering & structural dynamics*, 34(1):1–20, 2005. Publisher: Wiley Online Library.

[7] Roger E. Scholl. Observations of the performance of buildings during the 1985 Mexico earthquake, and structural design implications. *International Journal of Mining and Geological Engineering*, 7(1):69–99, March 1989.

[8] C Arnold. Pounding damage at hotel de carlo. *The Earthquake Engineering Online Archive NISEE e-Library*, 1985.

[9] H Sezen. Note effect on pounding. *The Earthquake Engineering Online Archive NISEE e-Library*, 1999.

[10] Brussels European Committee for Standardization. Design of structures for earthquake resistance. part 1: General rules, seismic actions and rules for buildings. en 1998-1. *Eurocode 8*, 2004.

[11] Jack Moehle and Gregory Deierlein. A framework methodology for performance-based earthquake engineering. January 2004.

[12] Jack W Baker. Introduction to Probabilistic Seismic Hazard Analysis. page 79, 2008.

[13] Sushil Khatiwada and Nawawi Chouw. Limitations in Simulation of Building Pounding in Earthquakes. *International Journal of Protective Structures*, 5(2):123–150, June 2014. Publisher: SAGE Publications.

[14] Michel Jean. The non-smooth contact dynamics method. *Computer Methods in Applied Mechanics and Engineering*, 177(3-4):235–257, 1999. Publisher: Elsevier.

[15] Vincent Acary. *Contribution à la modélisation mécanique et numérique des édifices maçonnés*. phdthesis, Université de la Méditerranée - Aix-Marseille II, May 2001.

[16] Vincent Crozet. *Etude de l'entrechoquement entre bâtiments au cours d'un séisme*. These de doctorat, Institut polytechnique de Paris, November 2019.

[17] J. J. Moreau. Standard Inelastic Shocks and the Dynamics of Unilateral Constraints. In Gianpietro Del Piero and Franco Maceri, editors, *Unilateral Problems in Structural Analysis*, International Centre for Mechanical Sciences, pages 173–221, Vienna, 1985. Springer.

[18] Vincent Acary. Energy conservation and dissipation properties of time-integration methods for nonsmooth elastodynamics with contact. *ZAMM - Journal of Applied Mathematics and Mechanics / Zeitschrift für Angewandte Mathematik und Mechanik*, 96(5):585–603, 2016. _eprint: https://onlinelibrary.wiley.com/doi/pdf/10.1002/zamm.201400231.

[19] S. Castro, Crempien J. Benavente, R., G. Candia, and J.C. de la Llera. A consistently processed strong motion database for chilean earthquakes. 90, 2021. Submitted.

[20] Nicolas Luco and C. Allin Cornell. Structure-Specific Scalar Intensity Measures for Near-Source and Ordinary Earthquake Ground Motions. *Earthquake Spectra*, 23(2):357–392, May 2007.

[21] Laura Eads, Eduardo Miranda, Helmut Krawinkler, and Dimitrios G. Lignos. An efficient method for estimating the collapse risk of structures in seismic regions: an efficient method for estimating the collapse risk of structures. *Earthquake Engineering & Structural Dynamics*, 42(1):25–41, January 2013.

[22] Laura Eads, Eduardo Miranda, and Dimitrios G. Lignos. Average spectral acceleration as an intensity measure for collapse risk assessment: Average Spectral Acceleration as an IM for Collapse Risk Assessment. *Earthquake Engineering & Structural Dynamics*, 44(12):2057–2073, September 2015.

[23] Marco de Biasio. Ground motion intensity measures for seismic probabilistic risk analysis. page 169, 2014.